Available online at www.sciencedirect.com
SCIENCE DIRECT®
Earth and Planetary Science Letters 218 (2004) 363–377
EPSL
www.elsevier.com/locate/epsl

Modelling Pliocene warmth: contribution of atmosphere, oceans and cryosphere

Alan M. Haywood *, Paul J. Valdes

Department of Meteorology, The University of Reading, Earley Gate, PO Box 243, Whiteknights, Reading RG6 6BB, UK

Received 1 May 2003; received in revised form 1 October 2003; accepted 25 November 2003

Abstract

The relative role of the atmosphere, oceans and cryosphere in contributing towards middle Pliocene warmth (ca 3 Ma BP) is investigated using the HadCM3 coupled ocean–atmosphere general circulation model. The model was initialised with boundary conditions from the USGS PRISM2 data set and a Pliocene atmospheric CO_2 level of 400 ppmv and run for 300 simulated years. The simulation resulted in a global surface temperature warming of 3°C compared to present-day. In contrast to earlier modelling experiments for the Pliocene, surface temperatures warmed in most areas including the tropics (1–5°C). Compared with present-day, the model predicts a general pattern of ocean warming (1–5°C) in both hemispheres to a depth of 2000 m, below which no significant differences are noted. Sea ice coverage is massively reduced (up to 90%). The flow of the Gulf Stream/North Atlantic Drift is up to 100 mm s^{-1} greater in the Pliocene case. Analysis of the model-predicted meridional streamfunction suggests a global pattern of reduced outflow of Antarctic bottom water (AABW; up to 5 Sv), a shallower depth for North Atlantic deep water formation and weaker thermohaline circulation (3 Sv). The decrease in AABW occurs mainly in the Pacific rather than Atlantic Ocean. Model diagnostics for heat transports indicate that neither the oceans nor the atmosphere are transporting significantly more heat in the Pliocene scenario. Rather, these results indicate that the major contributing mechanism to global Pliocene warmth was the reduced extent of high-latitude terrestrial ice sheets (50% reduction on Greenland, 33% reduction on Antarctica) and sea ice cover resulting in a strong ice-albedo feedback. These results highlight the need for further studies designed to improve our knowledge regarding Pliocene terrestrial ice configurations.

Keywords: Pliocene; general circulation model; ocean; atmosphere; forcing

1. Introduction

The middle Pliocene (ca 3 Ma BP) represents a recent period in geological history when the climate of the Earth was significantly warmer than present-day. The period has been studied extensively by palaeoenvironmental/climatologists. Geological data supporting the assertion of a

* Corresponding author. Present address: Geological Sciences Division, British Antarctic Survey, High Cross, Madingley Road, Cambridge, CB3 0ET, UK.
Fax: +44-1223-362616.
E-mail address: ahay@bas.ac.uk (A.M. Haywood).

0012-821X/03/$ – see front matter © 2003 Elsevier B.V. All rights reserved.
doi:10.1016/S0012-821X(03)00685-X

warmer than present climate includes sea surface temperatures (SSTs) reconstructed from planktonic foraminifera [1–5], ostracods [6,7], siliceous microfossil records [8], diatom records [9], terrestrial vegetation records [10–12] and numerous records of higher than present sea levels [13–15].

Numerous modelling studies have been conducted for the period. The first study used the PRISM0 8°×10° digital data set and the GISS (Goddard Institute for Space Studies) atmospheric general circulation model (GCM; 8°×10° model resolution) which focussed on the middle Pliocene climate of the Northern Hemisphere [16]. The second model investigation used a 2°×2° version of the (PRISM1) digital data set to prescribe the boundary conditions for the NCAR (National Centre for Atmospheric Research) GENESIS atmospheric GCM (4.5°×7.5° model resolution) which examined the nature of the middle Pliocene climate on a global scale [17]. A global scale palaeoclimate reconstruction for the middle Pliocene was conducted using the updated PRISM2 digital data set and the UKMO (United Kingdom Meteorological Office) atmospheric GCM, running with an enhanced spatial resolution of 2.5°×3.75° [18]. The same model has been used to carry out detailed data/model comparisons on a regional scale [19,20] and to conduct ice sheet sensitivity/biome experiments for the period [21–23].

Despite these modelling studies, the cause of middle Pliocene warmth continuous to be the subject of much debate [16,17,24–27]. A combination of modelling studies and evidence from Pliocene proxy data indicate that CO_2 concentrations at 3 Ma BP were greater (absolute value 400 ppmv) compared to mid-19th century levels (~280 ppmv) [28,29,25,30,31]. However, an increase in CO_2 alone would be expected to raise surface temperatures at all latitudes, and, hence, cannot explain the reconstructed pattern of little or no SST change at the equator [2–4].

Variations in oceanic circulation and increased heat advection away from the equator to high latitudes have been proposed as a significant causal factor in producing the climate of the middle Pliocene [25,26,3]. Such an increase in heat advection could be a response to enhanced thermohaline circulation in the oceans or enhanced surface gyre flow resulting from increased regional atmospheric winds and wind stresses [19]. Thus far, all palaeoclimate modelling studies of the middle Pliocene have been restricted to using atmospheric GCMs utilising prescribed SSTs and/or a simple slab-ocean model [32,22]. Although slab-ocean models are capable of simulating part of the feedbacks of the oceans on climate, they are incapable of simulating changes to horizontal ocean heat transports, and related changes to ocean currents and thermohaline circulation. These have been recognised as potentially pivotal mechanisms in forcing climate change for the Pliocene and many other time periods [33–35].

Thus it has not been possible to robustly examine the oceans role in generating and or maintaining mid-Pliocene warmth. This study aims to remedy this situation through the use of a fully coupled atmosphere–ocean model.

2. Model description, experimental design and boundary conditions

2.1. The UKMO GCM

The particulars of the version of the UKMO GCM (hereafter referred to as HadCM3) used in this study are well documented [36]. However, some discussion of the model itself and how HadCM3 differs from HadCM2 is necessary. HadCM3 was developed at the Hadley Centre for Climate Prediction and Research, which is a part of the UK Meteorological Office. The model is one of a new breed of coupled ocean–atmosphere GCMs (OAGCM) that requires no flux corrections to be made, even for simulations of a thousand years or more [37]. The GCM consists of a linked atmospheric model, ocean model and sea ice model. The horizontal resolution of the atmospheric model is 2.5° in latitude by 3.75° in longitude. This gives a grid spacing at the equator of 278 km in the north–south direction and 417 km east–west and is approximately comparable to a T42 spectral model resolution. The atmospheric model consists of 19 layers. The spatial resolution over the ocean is improved in HadCM3 to

1.25°×1.25° and the model has 20 layers. The atmospheric model has a timestep of 30 min and includes a new radiation scheme that can represent the effects of minor trace gases [38]. A parameterisation of simple background aerosol climatology is also included [39]. The convection scheme has also been improved [40]. A new land-surface scheme includes the representation of the freezing and melting of soil moisture. The representation of evaporation now includes the dependence of stomatal resistance on temperature, vapour pressure and CO_2 concentration [41].

Significant changes in the ocean model include the use of the Gent–McWilliams mixing scheme [42]. There is no explicit horizontal tracer diffusion in the model. The improved horizontal resolution allows the use of a smaller coefficient of horizontal momentum viscosity leading to an improved simulation of ocean velocities. The sea ice model is, in large part, the same as that employed within HadCM2. It uses a simple thermodynamic scheme and contains parametrisations of ice drift and leads [43].

The above changes have resulted in a much improved SST and sea ice climatology compared to earlier generations of the model, whilst the atmospheric part of the model is capable of a realistic simulation of the surface heat flux.

2.2. Experimental design

Two coupled ocean–atmosphere experiments have been conducted, one for present-day and one for the middle Pliocene. A CO_2 concentration of 400 ppmv is used in the Pliocene coupled run which represents an estimate in line with proxy evidence [25,30,31], whilst the present-day coupled run has a mid-19th century level of CO_2 (~280 ppmv). The Pliocene coupled run is compared to both the present-day coupled simulation and a Pliocene fixed SST experiment using only the atmospheric component of the HadCM3 GCM and the PRISM2 SSTs [18]. The coupled simulation for the Pliocene was integrated over 300 years with climatological means being derived from the final 60 simulated years. For the Pliocene fixed SST experiment, the model was integrated for 12 simulated years with climatological means being derived from the final 10 years only. For further details of the model set up for the fixed SST experiment, see [18].

The Pliocene coupled experiment was initialised with boundary conditions derived from the PRISM2 digital data set (see Section 2.3). The surface ocean was initialised with monthly SSTs derived from PRISM2. For the first 30 years of the model integration, a simple Haney restoring term fixed the model-predicted SSTs to the PRISM2 SST reconstruction and sea surface salinity (SSS) to the present-day value. However, after 30 simulated years the Haney function was gradually reduced to zero, after which the model was completely free to simulate changes in SST and SSS.

2.3. Middle Pliocene boundary conditions

For this modelling study the required boundary conditions were supplied by the United States Geological Survey (USGS) PRISM2 enhanced 2°×2° digital data set (Pliocene Research Interpretations and Synoptic Mapping). The particulars of the PRISM2 data set have been well documented in previous papers [4,18]. In brief, the prescribed boundary conditions cover the time slab between 3.29 and 2.97 Ma BP according to the geomagnetic polarity time scale [44]. Boundary conditions integrated into the model that are specific to the middle Pliocene include: (1) continental configuration, modified by a 25 m increase in global sea level, (2) modified present-day elevations, (3) reduced ice sheet size and height for Greenland (~50% reduction) and Antarctica (~33% reduction), (4) Pliocene vegetation distribution and (5) Pliocene SSTs and sea ice distributions (used to spin up the ocean for the first 30 simulated years only in the coupled runs but were used in the Pliocene fixed SST experiment). The 25 m sea level rise is equivalent to a maximum decrease in global average salinity of approximately 0.25 psu, which is small and therefore was not included in the simulation. The reader is referred to the following USGS open file report (http://pubs.usgs.gov/openfile/of99-535/) for a more detailed description of the new PRISM2 data set which fully documents the construction

of PRISM2 and how it differs from earlier PRISM data sets [4].

For the Pliocene fixed SST experiment, the land/sea mask was reconfigured to match that provided by PRISM2 [18]. However, due to the resolution of the atmospheric component of the GCM (2.5°×3.75°), this meant that only a dozen grid points required alteration. Therefore, in the Pliocene coupled experiment the land/sea mask for present-day was retained.

3. Results (*atmosphere*)

3.1. Surface temperature (°C)

The global average surface temperature for the Pliocene coupled experiment is equal to 18.27°C which represents a positive ΔT of 3.09°C compared to the coupled experiment for present-day. Compared to the Pliocene fixed SST experiment the global annual average surface temperature in the coupled experiment is 1.64°C warmer. Average warming compared to the present-day coupled and fixed SST simulation over land is equal to 4.2 and 2.21°C. Over the oceans this changes to 3.35 and 0.8°C respectively. The equator-to-pole temperature gradient is reduced by 9.04°C compared to the present-day coupled experiment but increased by 1.81°C in comparison with the Pliocene fixed SST simulation. The largest magnitude of surface temperature warming compared to present-day occurs in the high latitudes over areas occupied by terrestrial ice sheets/

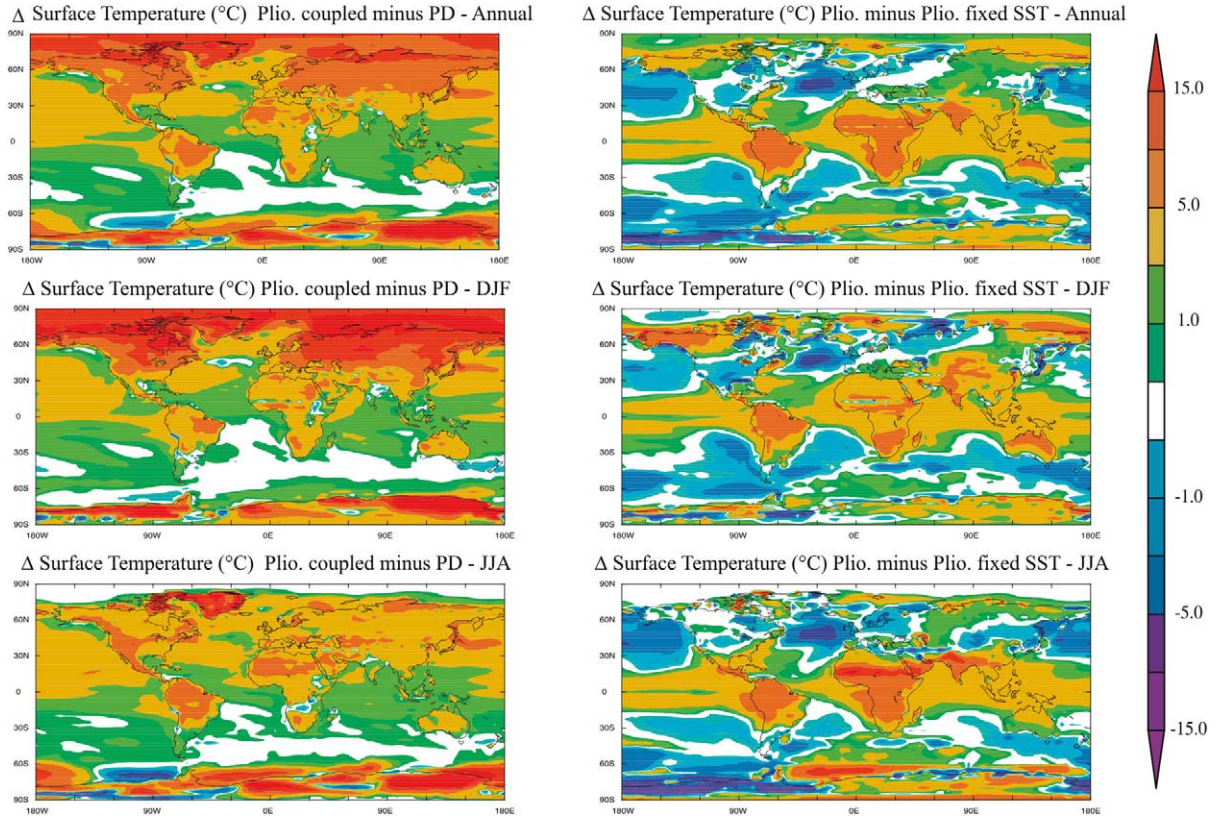

Fig. 1. Model predictions for surface temperature (°C). From top left to bottom right: difference between Pliocene coupled and present-day coupled experiment as an annual mean; difference between Pliocene coupled and Pliocene fixed SST as an annual mean; difference between Pliocene coupled and present-day coupled for DJF; difference between Pliocene coupled and Pliocene fixed SST for DJF; difference between Pliocene coupled and present-day coupled for JJA; difference between Pliocene coupled and Pliocene fixed SST for JJA.

sea ice (Fig. 1). The greatest warming at high latitudes occurs in the winter hemisphere and is associated with changes in the cryosphere. In the tropics and mid-latitudes, a ΔT of +3 to +5°C compared to present-day, is common over terrestrial regions in both the annual mean and seasonally. Larger changes ($\Delta T = 5$ to 10°C) are predicted over the western cordillera of North America and in the Amazonian region of Brazil.

Over the oceans, surface temperature increases between 1 and 5°C compared to present-day. This pattern remains stable over the seasonal cycle. No surface temperature increase is predicted in certain areas of the South Atlantic and Southern Ocean both annually and seasonally.

The predicted high-latitude warming is principally a reflection of the smaller land ice sheets prescribed from the PRISM2 data set. This forces a substantial change in the surface and planetary albedo, which subsequently leads to a reduction in sea ice coverage and sea ice depth in both hemispheres. Higher sea levels also act as an important positive feedback mechanism on high-latitude climate since oceans cool to a lesser degree than land areas. Warming over the western cordillera of North and South America is linked to the lower prescribed orography of these regions ($\sim$50% of modern) specified from the PRISM2 data set. The enhanced CO_2 level, in part, drives surface temperature warming over the tropics in the Pliocene coupled experiment. Changes in tropical SSTs, cloud cover and the precipitation/evaporation feedback also represent important feedback mechanisms on tropical temperatures. Over the Amazon, the warming is associated with reduced precipitation rates that are themselves driven by enhanced trade wind flow. Over North Africa, warming is generated by enhanced tropical SSTs and CO_2 increases.

Compared to the fixed SST experiment, surface temperatures in the Pliocene coupled run are generally warmer in equatorial regions (between 1 and 10°C) and cooler in the mid-latitudes, particularly over the North Atlantic region (Fig. 1). This pattern remains constant over the seasonal cycle. The pattern of change in the tropics is driven by a complex set of forcing and feedback mechanisms. Enhanced CO_2 accounts for only a small part of the signal of warming observed. Combined with this, the altered SST pattern predicted in the Pliocene coupled run forces changes (weakens) to the strength of Hadley circulation and the width (narrows) of the Hadley Cell which reduces rainfall, decreases evaporation and latent heat flux from the land and hence raises surface temperatures. The cooling predicted at mid-to-high latitudes is primarily forced by variations in SSTs.

3.2. Total precipitation rate (mm/day)

The global average precipitation rate for the Pliocene coupled simulation is equal to 3.13 mm/day. This represents only a small increase from the present-day coupled experiment of 0.13 mm/day (4%) and is almost identical to results from the fixed SST experiment ($\sim$3.01 mm/day). Total precipitation rates averaged over land and the oceans are equal to 2.55 and 3.44 mm/day respectively, which is again almost identical in the present-day and the Pliocene fixed SST simulations.

As an annual mean and seasonally, significant differences are predicted in the spatial distribution of precipitation between the Pliocene and present-day coupled experiments. In the Northern Hemisphere at mid-to-high latitudes, annual mean precipitation rates increase by an average of 0.2 to 2 mm/day. The increase in mid-latitude precipitation is associated with enhanced surface temperatures predicted in the Pliocene control experiment. This pattern is not mirrored in the Southern Hemisphere largely due to the lower magnitude of surface temperature change. Precipitation rates decrease over areas of central and Southwest USA and the western and eastern Mediterranean Basins by a maximum of 1 mm/day. The latter difference is related to a shift in the position of the winter storm track and associated enhancement of the Azores high-pressure system. This acts to block Atlantic depressions from entering the Mediterranean and instead diverts the precipitation across NW Europe. This pattern is akin in many respects to the North Atlantic Oscillation in a positive phase.

In general the largest predicted differences in

precipitation rate occur in tropical regions. During JJA (June, July and August), precipitation rates over the northern Indian Ocean and India itself increase by a maximum of 4 mm/day, suggesting an enhanced South Asian summer monsoon in the Pliocene case (linked to the enhanced warming of Eurasia). At equatorial and low latitudes decreases in precipitation over North Africa during JJA (0.2–2 mm/day) are predicted, indicating a West African monsoon of reduced strength (Fig. 2). Over Central and Latin America/South America, annual mean precipitation rate decreases by 0.2 to <4 mm/day. This pattern is constant through the seasonal cycle and represents one of the most spatially extensive changes between the Pliocene and present-day coupled experiments. This response is a function of the altered Atlantic SST distribution and temperature gradients in the Pliocene coupled simulation. Over the equatorial Pacific, annual mean precipitation rates increase by more than 4 mm/day. This response is a function of the warmer SSTs predicted in this region.

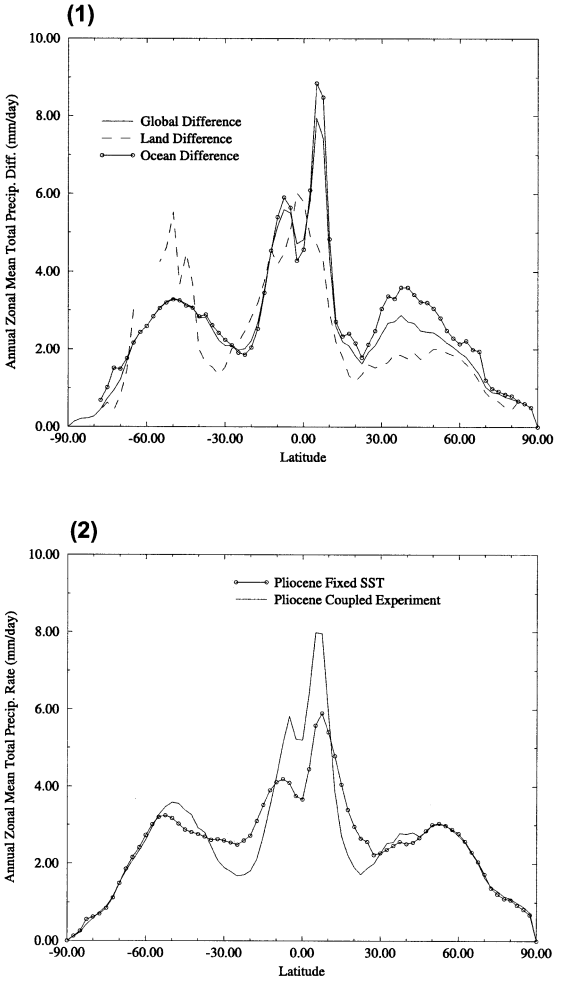

Fig. 2. (1) Difference in annual zonal mean total precipitation rate (mm/day) between the Pliocene coupled and present-day coupled experiments averaged globally, over land and ocean regions. (2) Annual zonal mean total precipitation rate (mm/day) for the Pliocene fixed SST experiment and the Pliocene coupled experiment.

Compared to the Pliocene fixed SST experiment, total precipitation rates in the Pliocene coupled experiment are reduced by 2 mm/day as an annual mean over the North Atlantic and by <4 mm/day during DJF (December, January and February). This reduction is associated with the lower SSTs predicted by the model over this region. Large reductions in precipitation rate are also noted in the equatorial Atlantic, Central/Latin America, northern South America, North Africa and the Mediterranean both annually and seasonally (<4 mm/day). These changes are caused by altered storm tracks, SST distributions and a narrower model-predicted Hadley cell/weaker Hadley circulation in these areas (Fig. 2). Over the tropical Pacific, Indian Ocean and Indonesian region precipitation rates increase by more than 4 mm/day. This is primarily a response to the warmer SSTs predicted in these regions in the Pliocene coupled experiment.

4. Results (*ocean*) Pliocene coupled vs present-day coupled experiment

4.1. Ocean temperatures (°C)

As an annual zonal average, SSTs in the Pliocene coupled experiment are 2.2°C warmer than the present-day case. The spatial difference in annual and seasonal SSTs between the Pliocene coupled, present-day coupled and Pliocene fixed SST experiments are shown in Fig. 1. Compared to present-day, SSTs are warmer in the low and mid-latitudes by an average of 1–5°C. At high latitudes SST warming is predicted to be

5–10°C, which is indicative of a reduced sea ice coverage and depth in the Pliocene case. This pattern of SST change remains constant over the seasons. No increase in SST is predicted between the Pliocene coupled and present-day coupled experiments in areas of the Southern Ocean.

The absolute zonal mean ocean temperatures and differences between the zonal mean ocean temperature for the Pliocene and present-day are shown in Fig. 3. Differences in latitude/longitude depth profiles for ocean temperature are also presented. As an annual zonal mean, ocean temperatures are, on average, 1–5°C warmer in the Pliocene coupled experiment compared to present-day to a depth of 2000 m. This trend is particularly robust at mid to high latitudes in the Northern Hemisphere. At low latitudes and in the Southern Hemisphere ocean warming is of the order of 1–3°C to a depth of 2000 m. Below 2000 m, little difference in ocean temperature is predicted between the Pliocene and present-day coupled experiments. The only change predicted is a reduction of ocean temperatures by 0.5°C to 2°C around 75°N deeper than 2000 m. This change is related to a shallowing in North Atlantic deep water formation (NADW) in the Pliocene case.

As a latitudinal depth profile through the ocean at 30°W, the model predicts increased ocean temperatures in the surface layer to a depth of 2500 m below which ocean warming becomes sporadic (Fig. 3). The magnitude of this warming is greatest in the surface and near-surface layers of the ocean and gradually decreases with depth. Greater ocean warming is predicted along this transect in the Northern Hemisphere (~1–5°C) as compared to the Southern Hemisphere (~1°C).

As a longitudinal depth profile through 0°N, the model predicts increased ocean temperatures of 1–5°C to a depth of 1200 m (Fig. 3). Below 1200 m little significant difference in ocean tem-

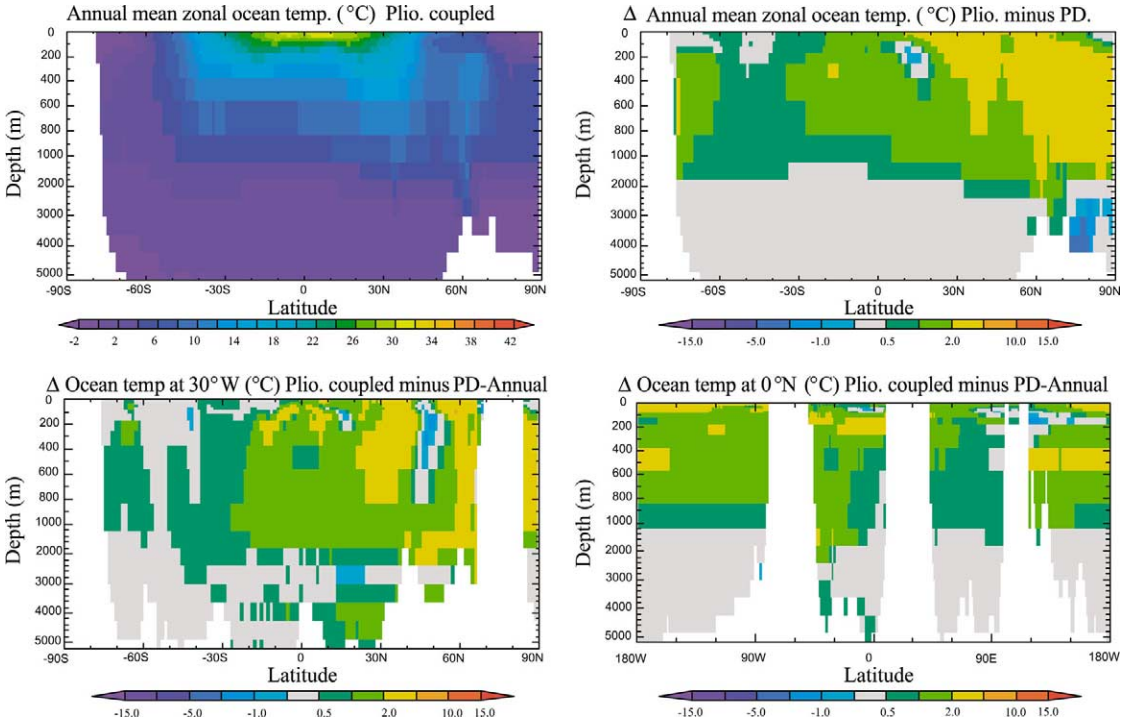

Fig. 3. Plots of annual mean characteristics of ocean temperature (°C) for the Pliocene coupled experiment versus the present-day coupled experiment. From top left to bottom right: annual zonal mean ocean temperature for the Pliocene coupled experiment; difference between Pliocene and present-day annual zonal mean temperatures; difference between Pliocene and present-day ocean temperature shown as a latitudinal cross section spanning 30°W; difference between Pliocene and present-day ocean temperatures shown as a longitudinal cross section spanning 0°N.

peratures between the Pliocene and present-day is predicted.

4.2. Mixed layer depth (m) and salinity (psu)

The depth of the mixed layer as an annual mean is similar in both the present-day and Pliocene coupled experiments with the following exceptions. In the Northern Hemisphere, the mixed layer increases in depth by 10–50 m in the North Atlantic in areas south of Iceland. An increase in the mixed layer of 10–100 m is predicted in the Northern Hemisphere between 30 and 60°E and approximately 75°N. This increase in the mixed layer is related to surface temperature increases in the same region related to the reduction in the depth and coverage of Arctic sea ice in the Pliocene coupled experiment. The pattern of change noted in the Northern Hemisphere is not mimicked in the Southern Hemisphere where no consistent pattern of either deepening or shallowing of the mixed layer is predicted.

Model-predicted changes in ocean salinity (psu) indicate that the deepening of the mixed layer in areas of the North Atlantic and Arctic Ocean are associated with enhanced ocean salinities (1–5 psu). This is caused by (a) the simulated higher-latitude warming in the Pliocene case and (b) the reduced sea ice cover (as much as 90% in the Arctic), which enhances evaporation ($\sim$1 mm/day as an annual mean, $\sim$4 mm/day during DJF) from the ocean. Enhancements in seasonal ocean salinity north of Iceland are also driven by sea ice formation and decay and associated processes of brine rejection. However, since ocean salinity is enhanced more during JJA in this region, when sea ice coverage is lowest, we conclude that the dominant control in increasing salinity north of Iceland is enhanced evaporation from the ocean surface rather than brine rejection from sea ice.

4.3. Sea ice coverage (%) and depth (m)

In response to the simulated high-latitude warming, particularly in the winter hemisphere, sea ice coverage and sea ice depth in the Pliocene coupled experiment is significantly reduced compared to present-day. During DJF, sea ice coverage may be reduced by as much as 90% in the Northern Hemisphere whereas sea ice depth is on average reduced by 1–4 m. The largest magnitude of sea ice depth reduction occurs off the coast of East Greenland (1–5.5 m). In the Southern Hemisphere during DJF both sea ice coverage and depth are reduced but by a smaller magnitude (on average 10 – 50% and 1 – 2.5 m respectively). During JJA, sea ice coverage and depth decrease more substantially in the Southern Hemisphere compared to DJF. However, the predicted reductions are of a similar magnitude as those simulated for the Northern Hemisphere during JJA. In both hemispheres sea ice coverage is reduced by an average 1–50%. Sea ice depth is reduced by an average 1–3 m. The reduction in sea ice is produced primarily by the warmer SSTs simulated by the model in the Pliocene case.

Within the PRISM2 data set, the Arctic is estimated to be seasonally ice free [4]. This assertion is supported by foraminifer, ostracod and mollusc data [45,46]. The Pliocene model results concur that during August, September and October the Arctic becomes ice free. Furthermore, the model predicts that Antarctic sea ice is lost almost entirely during the Southern Hemisphere summer season.

4.4. Surface ocean current strength (mm s^{-1})

Numerous significant differences in ocean surface current strength are predicted between the Pliocene and present-day coupled experiments. Of first order importance is the model representation of the western (poleward flowing) and eastern (equatorward flowing) boundary currents. As an annual mean, the strength of both Gulf Stream and Kuroshio Currents increases by a maximum of 300 mm s^{-1} compared to present-day (Fig. 4). Other currents comprising the North Atlantic gyre (e.g. Canaries, Antilles, and Florida Currents) show little variation in terms of flow direction and strength from the present-day scenario. Southward flow strength of the East Greenland and Labrador Currents increases by a maximum of 300 mm s^{-1} compared to present-day. These changes are the result of the model-predicted in-

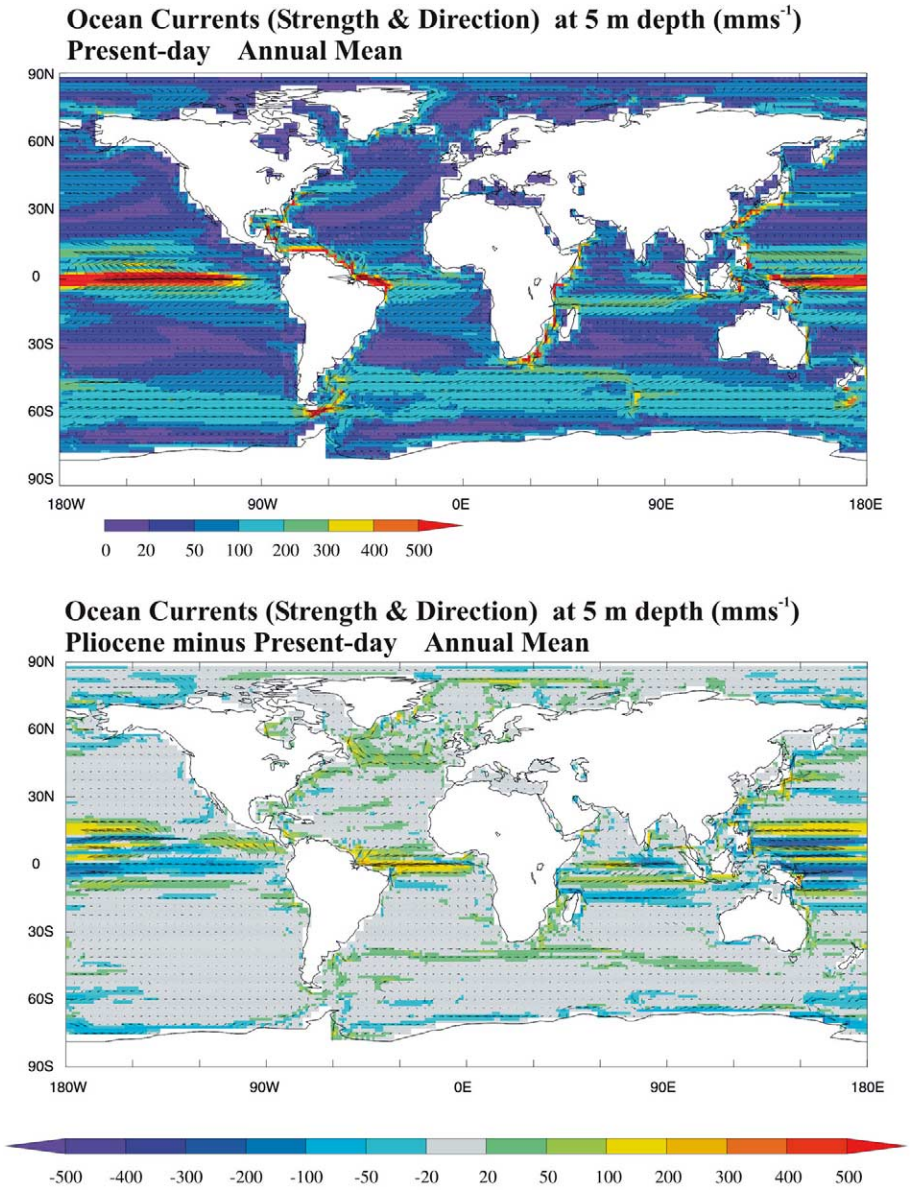

Fig. 4. Showing absolute ocean current strengths (mm s^{-1}) and direction of ocean currents simulated for the present-day and the difference in the strength and direction of ocean currents between the Pliocene and present-day coupled experiments. Note the increase in flow speed of the Gulf Stream/North Atlantic Drift, increased flow of Greenland and Labrador Currents in the Pliocene scenario.

crease in westerly wind strength/stress over the North Atlantic.

In the Pacific, the North Pacific and California Currents show little change from modern and may weaken by 50 mm s^{-1}. The model predicts that the southward flowing Oyashio Current does not, unlike the East Greenland Current, increase in strength. In fact a moderate weakening of this current is predicted ($\sim$50–100 mm s^{-1}). The North Equatorial Current is enhanced in flow speed by 200 mm s^{-1}. The Equatorial Counter Current is simulated as being reduced in strength

by up to 100 mm s^{-1}, whereas the flow of the South Equatorial Current appears moderately enhanced by 50 mm s^{-1} compared to the modern.

In the South Atlantic, the Guinea Current is predicted to be unchanged in the Pliocene experiment. The strength of the Benguela and Brazil Currents also appears to be little different (or slightly weaker by ~0–50 mm s^{-1}) from present-day, whereas the flow of the Falklands Current is up to 100 mm s^{-1} stronger in the Pliocene experiment (Fig. 4). In the South Pacific, the strength of the Peru Current (Humboldt) is simulated as being no different, or slightly weaker (~50–100 mm s^{-1}), than present-day. The flow of the Antarctic circumpolar current is generally the same or slightly weaker in strength compared to present by 20–50 mm s^{-1}. In the Indian Ocean, the Agulhas Current is up to 100 mm s^{-1} stronger in the Pliocene scenario.

4.5. Meridional overturning streamfunction (Sv)

The difference in meridional overturning streamfunction between the Pliocene and present-day coupled experiment is complex. As a global mean, differences indicate that for the Pliocene coupled experiment the flow of Antarctic bottom water (AABW) is reduced by a maximum of 5 Sv (Fig. 5). The rate of downwelling in the Northern Hemisphere also appears to be reduced by up to 3 Sv. For the Atlantic sector, the results indicate that, in the Pliocene case, AABW flow is either

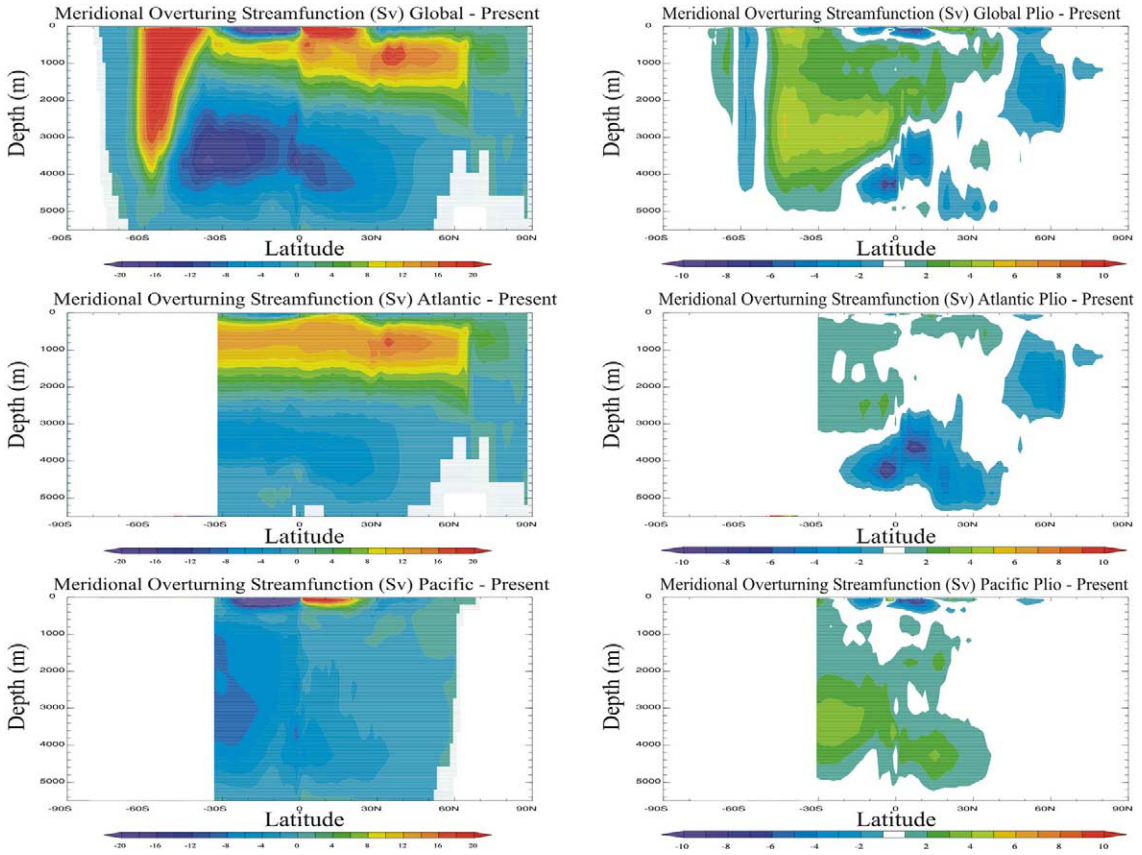

Fig. 5. HadCM3 GCM predictions of absolute meridional overturning streamfunction (Sv) for the present-day coupled experiment averaged over the globe and the Atlantic and Pacific Oceans, and the difference between the Pliocene coupled and present-day coupled meridional overturning streamfunction.

the same as, or locally slightly stronger than (1 to 6 Sv), present-day. However the strength and depth of the North Atlantic thermohaline circulation is reduced. For the Pacific Ocean, the only significant change predicted is a reduction in AABW flow by 4 Sv (Fig. 5).

These results imply both a shallowing and reduction in the strength of the thermohaline circulation, and a reduction in AABW flow mainly in the Pacific Ocean in the Pliocene case.

5. Discussion

5.1. Forcing of oceans, atmosphere and cryosphere on Pliocene warmth

Numerous proposals exist within the literature to account for the relative climatic warmth of the middle Pliocene. These include increased concentrations of CO_2 [31], enhanced thermohaline circulation [25], a more vigorous flow of surface ocean gyres [19,47], alterations in the outflow of Antarctic deep water [27], and changes in the elevations of mountain chains [48]. All of these explanations have weaknesses when examined in detail and there may have been numerous contributing factors to middle Pliocene warmth. For example, it has been suggested that the warmth was generated through a combination of enhanced atmospheric CO_2 and an increase in thermohaline circulation [25]. What significance do the new coupled OAGCM results presented in this paper have to established ideas concerning the genesis of Pliocene warmth?

In order to better understand the model response for the Pliocene it is interesting to consider the global annual average radiative balance. Increasing CO_2 from 280 to 400 ppmv produces a forcing of 1.9 W m^{-2}. However, the surface albedo has also been affected as a result of the reduced ice cover in Greenland and Antarctica. Furthermore, the model predicts reduced snow and sea ice cover for the Pliocene. This results in a change in the top of the atmosphere solar flux (excluding clouds) of 2.3 W m^{-2}. By examining the surface albedo, approximately 55% of this change is due to the terrestrial ice and 45% from sea ice. Changes in snow cover are almost of negligible importance. Finally we also calculated the changes in cloud radiative forcing. This shows that the changes in cloud cover acted as a strong positive feedback, contributing 1.8 W m^{-2} to the overall forcing. This latter result is potentially very model dependent, clouds being one of the most uncertain aspects of climate models.

The forcing by CO_2 and by the cryosphere changes are more confident from an internal modelling perspective. However, both are highly uncertain for the Pliocene. Fig. 6 shows difference in model-predicted northward heat transport by the atmosphere and oceans between the present-day and Pliocene coupled experiments. The figure dramatically highlights the insignificant changes in atmospheric and oceanic heat transports for the Pliocene. In effect, neither the atmosphere nor the oceans are actively 'working harder' in the Pliocene scenario. On the basis of these results it is clear that the reduced volume of land ice cover is an important forcing mechanism on Pliocene climates with sea ice cover, ocean temperatures and subsequently atmospheric temperatures responding to the forcing delivered by the cryosphere.

The apparent significance of the imposed Pliocene terrestrial ice configuration within the coupled modelling raises an interesting question

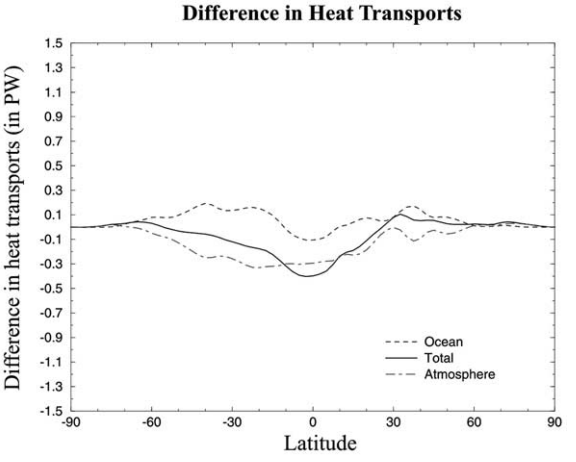

Fig. 6. Model-predicted difference in poleward heat transports (PW) between the Pliocene coupled and present-day coupled model experiments using the HadCM3 GCM.

regarding the validity of the model experiment itself. Our knowledge of the Greenland and Antarctic ice sheets is without doubt the weakest area concerning Pliocene palaeoenvironmental conditions. On the basis of these results it is clear that significantly more modelling effort needs to be directed towards addressing the question of terrestrial ice volume for Antarctica. For example, if we assume that the PRISM2 reconstruction of Pliocene SSTs is accurate, a useful study would be to assess what global ice configuration would be in equilibrium with the given SSTs using an ice sheet model coupled to an atmosphere-only GCM. This would enable us to improve our understanding of how relevant the current ice configuration presented in PRISM2 is to other boundary conditions, such as SSTs, before conducting further computationally expensive coupled ocean–atmosphere experiments.

5.2. Model vs PRISM2 SSTs

Seventy-seven marine localities/sections were used to generate the PRISM2 SST reconstruction [4]. Included is an estimate of both winter and summer SSTs. PRISM therefore produced two primary Pliocene SST maps for the months of February and August. The remaining 10 months of the year were constructed by fitting a sine curve to the February and August SST estimates [3]. The distribution of PRISM marine data localities was also uneven and geographically incomplete. To produce a global SST data set, interpolation between data points was necessary. Therefore, the only robust form of comparison between the Pliocene coupled experiment and PRISM2 SST data is one carried out on a site-specific basis for February and August. Fig. 7 shows a series of three scatter graphs that plot model-predicted (from the

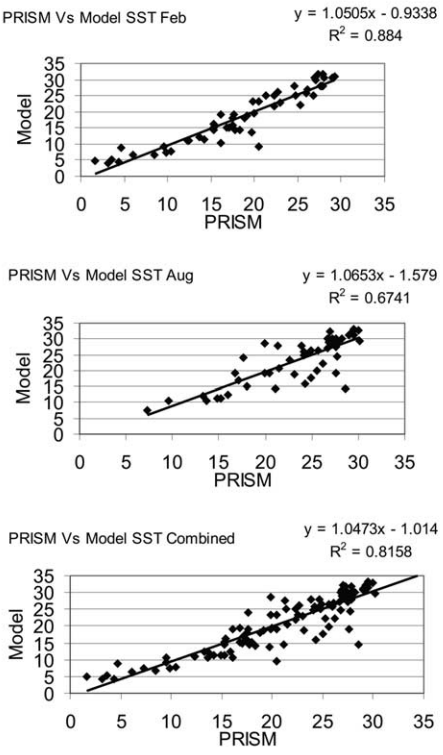

Feb
t-Test: Two-Sample Assuming Unequal Variances

	Variable 1	Variable 2
Mean	18.47055556	18.46888889
Variance	57.40754119	71.65988553
Observations	54	54
Hypoth. Mean Diff.	0	
df	105	
t Stat	0.001078046	
P(T<=t) one-tail	0.499570945	
t Critical one-tail	1.659495865	
P(T<=t) two-tail	0.999141889	
t Critical two-tail	1.982816684	

Aug
t-Test: Two-Sample Assuming Unequal Variances

	Variable 1	Variable 2
Mean	23.68388889	23.65148148
Variance	30.83689969	51.91099399
Observations	54	54
Hypoth. Mean Diff.	0	
df	100	
t Stat	0.026179581	
P(T<=t) one-tail	0.489583137	
t Critical one-tail	1.66023483	
P(T<=t) two-tail	0.979166275	
t Critical two-tail	1.983971742	

Combined Feb&Aug
t-Test: Two-Sample Assuming Unequal Variances

	Variable 1	Variable 2
Mean	21.07722222	21.06018519
Variance	50.56807632	67.98557754
Observations	108	108
Hypoth. Mean Diff.	0	
df	209	
t Stat	0.016261046	
P(T<=t) 1-tail	0.493520823	
t Critical one-tail	1.652176707	
P(T<=t) two-tail	0.98704167	
t Critical two-tail	1.971379788	

Fig. 7. Scatter plots for model-predicted February, August and combined February and August SSTs from the Pliocene coupled experiment versus the reconstructed February, August and combined February and August SSTs derived from the PRISM2 data set. Note: the degree of scatter is an estimate of similarity between data sets. The results from three *t*-tests assuming unequal variances on the data are also shown.

Pliocene coupled experiment) versus PRISM2 SSTs for February, August and February and August combined at each marine locality used by the PRISM Group. The results demonstrate that, as a whole, the SSTs predicted by the model and those reconstructed from geological data are not statistically different (at a 95% statistical significance level). An R^2 value of 0.88 for the month of February suggests that the two SST data sets are particularly similar. However, the degree of accordance reduces significantly for the August comparison ($R^2 = 0.67$). When February and August data are combined an R^2 value of 0.82 is obtained.

Although this statistical test indicates that, as a whole, the SST data sets for the Pliocene produced by the climate model and geological data are not statistically different, a number of anomalous data points are clearly evident. When these anomalous data points are plotted geographically, the North Atlantic and North Pacific are identified as regions where negative SST anomalies occur, particularly for August. The other clear trend is a positive SST anomaly between the model and data at equatorial and low latitudes in both February and August.

A more stringent comparison between model- and data-derived SST data sets can be achieved by plotting against one another the difference values of model-predicted and PRISM2 SSTs from a modern SST data set [49]. When done, any statistical similarity between the model results and data breaks down and the two data sets must be considered as significantly different. Therefore, on a site-to-site basis the model does not predict the same magnitude, or indeed sign, of SST change as is reconstructed from geological proxies.

The poor comparison of model versus data raises a number of issues related to both the model and the data. In most places, the discrepancy is smaller than the sum of the error bars associated with the modelling and the data. Model errors can arise from the poor representation of the internal physics of the model, missing processes, or incorrect boundary conditions. The first two sources of error potentially have widespread significance whereas the incorrect boundary conditions impact on the Pliocene modelling only.

As discussed in the previous section, the cause of the global warming during the Pliocene is strongly linked to changes in the cryosphere and feedbacks from clouds. The former represents a boundary condition and the latter represents internal physics of the model. Both are highly uncertain (but not necessarily incorrect) latitudinally. The model shows no change in heat transports. It is difficult to determine if this is the correct response, given the boundary conditions. In particular, the model shows relatively small changes in North Atlantic SSTs, whereas the data indicates considerable warming. The HadCM3 model has a relatively complete representation of the thermodynamics and hydrological processes which influence the thermohaline circulation but there are always possible errors. In addition, the effects of iceberg discharge are poorly represented. Additional model simulations using alternative parameterised physics and/or models would facilitate further clarification of this issue.

6. Conclusions

This paper presents the results from the first-ever coupled OAGCM model experiment for the middle Pliocene using the HadCM3 and the USGS PRISM2 data set. The model was integrated for 300 simulated years and used a Pliocene atmospheric CO_2 concentration of 400 ppmv.

- The simulation resulted in an increase in the global surface temperatures of 3°C compared to present-day.
- In contrast to earlier Pliocene modelling experiments using fixed SSTs or a slab-ocean, surface temperature warming occurred over all latitudes including the tropics.
- Oceans warmed on average by 3–5°C to a depth of 2000 m below which small changes from modern were predicted.
- AABW flow was reduced by a maximum of 5 Sv in the Pliocene case.
- There was no observed increase in thermohaline circulation and little change in the surface ocean gyres.
- Dominant forcing on the climate was derived

from alterations in the cryosphere, but with strong positive feedbacks from clouds. The results indicate that studies designed to improve our knowledge regarding mid-Pliocene Antarctic Ice Sheet extent and which evaluate the suitability of the PRISM2 ice sheet in relation to other PRISM boundary conditions are necessary.

Acknowledgements

Dr Harry Dowsett and the United States Geological Survey's PRISM Group are noted for their kind support and encouragement. Dr Lisa Sloan is thanked for providing thoughtful comments on results from the Pliocene coupled modelling. Dr Samantha Cook is thanked for her assistance with the data/model comparison. The authors would like to acknowledge the help and kind assistance of Prof. B.W. Sellwood, Dr D. Seidov and an anonymous reviewer for providing useful comments and reviews which greatly improved the manuscript.*[BOYLE]*

References

[1] H.J. Dowsett, R.Z. Poore, Pliocene sea surface temperatures of the North Atlantic Ocean at 3.0 Ma, Quat. Sci. Rev. 10 (1991) 189–204.
[2] H.J. Dowsett, T.M. Cronin, R.Z. Poore, R.S. Thompson, R.C. Whatley, A.M. Wood, Micropaleontological evidence for increased meridional heat transport in the North Atlantic Ocean during the Pliocene, Science 258 (1992) 1133–1135.
[3] H.J. Dowsett, J. Barron, R. Poore, Middle Pliocene sea surface temperatures: a global reconstruction, Mar. Micropaleontol. 27 (1996) 13–26.
[4] H.J. Dowsett, J.A. Barron, R.Z. Poore, R.S. Thompson, T.M. Cronin, S.E. Ishman, S.E., D.A. Willard, Middle Pliocene paleoenvironmental reconstruction: PRISM2, USGS Open File Report 99-535 (1999) http://pubs.usgs.gov/openfile/of99-535.
[5] M.E. Raymo, The initiation of Northern Hemisphere glaciation, Annu. Rev. Earth. Planet. Sci. 22 (1994) 353–383.
[6] T.M. Cronin, Pliocene shallow water paleoceanography of the North Atlantic Ocean based on marine ostracodes, Quat. Sci. Rev. 10 (1991) 175–188.
[7] R.M. Forester, Pliocene-climate history of the Western United States derived from lacustrine ostracodes, Quat. Sci. Rev. 10 (1991) 133–146.
[8] J.J. Morley, B.A. Dworetzky, Evolving Pliocene-Pleistocene climate: A North Pacific perspective, Quat. Sci. Rev. 10 (1991) 225–238.
[9] J.A. Barron, Pliocene paleoclimatic interpretation of DSDP Site 580 (NW Pacific) using diatoms, Mar. Micropaleontol. 20 (1992) 23–44.
[10] R.S. Thompson, Pliocene environments and climates in the western United States, Quat. Sci. Rev. 10 (1991) 115–132.
[11] L. Heusser, J. Morley, Pliocene climate of Japan and environs between 4.8 and 2.8 Ma: A joint pollen and marine faunal study, Mar. Micropaleontol. 27 (1996) 86–106.
[12] R.S. Thompson, R.F. Fleming, Middle Pliocene vegetation: reconstructions, paleoclimatic inferences, and boundary conditions for climatic modeling, Mar. Micropaleontol. 27 (1996) 13–26.
[13] H.J. Dowsett, T.M. Cronin, High eustatic sea level during the Middle Pliocene: Evidence from the southeastern U.S. Atlantic Coastal Plain, Geology 18 (1990) 435–438.
[14] J. Brigham-Grette, Warm Pliocene high sea-level events in the Arctic Alaska, EOS Trans. Am. Geophys. Union, Spring Meeting 75 (1994) (Suppl.).
[15] V.A. Zubakov. I.I. Borzenkova, Global palaeoclimate of the late Cenozoic, Developments in Palaeontology and Stratigraphy, Vol. 12, Elsevier, Amsterdam, 1999, 456 pp.
[16] M. Chandler, D. Rind, R. Thompson, Joint investigations of the middle Pliocene climate II: GISS GCM Northern Hemisphere results, Glob. Planet. Change 9 (1994) 197–219.
[17] L.C. Sloan, T.J. Crowley, D. Pollard, Modeling of middle Pliocene climate with the NCAR GENESIS general circulation model, Mar. Micropaleontol. 27 (1996) 51–61.
[18] A.M. Haywood, P.J. Valdes, B.W. Sellwood, Global scale palaeoclimate reconstruction of the middle Pliocene climate using the UKMO GCM: initial results, Glob. Planet. Change 25 (2000) 239–256.
[19] A.M. Haywood, B.W. Sellwood, P.J. Valdes, Regional warming: Pliocene (3 Ma) paleoclimate of Europe and the Mediterranean, Geology 28 (2000) 1063–1066.
[20] A.M. Haywood, P.J. Valdes, B.W. Sellwood, J.O. Kaplan, H.J. Dowsett, Modelling middle Pliocene warm climates and environments of the U.S.A., Palaeontol. Electron. 4 (2001) http://palaeo-electronica.org/2001_1/climate/issue1_01.htm.
[21] A.M. Haywood, P.J. Valdes, B.W. Sellwood, J.O. Kaplan, Antarctic climate during the middle Pliocene: model sensitivity to ice sheet variation, Palaeogeogr. Palaeoclimatol. Palaeoecol. 182 (2002) 93–115.
[22] A.M. Haywood, P.J. Valdes, B.W. Sellwood, Magnitude of middle Pliocene climate variability: A palaeoclimate modelling study, Palaeogeogr. Palaeoclimatol. Palaeoecol. 188 (2002) 1–24.
[23] A.M. Haywood, P.J. Valdes, J.E. Francis, B.W. Sellwood, Global middle Pliocene biome reconstruction: A data/model synthesis, Geochem. Geophys. Geosyst. 3 (2002) DOI 10.1029/2002GC000358.
[24] H.J. Dowsett, R.S. Thompson, J.A. Barron, T.M. Cronin,

R.F. Fleming, S.E. Ishman, R.Z. Poore, D.A. Willard, T.R. Holtz, Joint investigations of the middle Pliocene climate I PRISM paleoenvironmental reconstructions, Glob. Planet. Change 9 (1994) 169–195.
[25] M.E. Raymo, B. Grant, M. Horowitz, G.H. Rau, Mid-Pliocene warmth: stronger greenhouse and stronger conveyor, Mar. Micropaleontol. 27 (1996) 313–326.
[26] T.J. Crowley, Pliocene climates: the nature of the problem, Mar. Micropaleontol. 27 (1996) 3–12.
[27] S.J. Kim, T.J. Crowley, Increased Pliocene North Atlantic Deep Water: Cause or consequence of Pliocene warming, Paleoceanography 15 (2000) 451–455.
[28] T.J. Crowley, Modeling Pliocene warmth, Quat. Sci. Rev. 10 (1991) 272–282.
[29] M.E. Raymo, G.H. Rau, Plio-Pleistocene atmospheric CO_2 levels inferred from POM δ13C at DSDP Site 607, EOS Trans. Am. Geophys. Union, Spring Meeting 73 (1992) (Suppl.).
[30] J. Van der Burgh, H. Visscher, D.L. Dilcher, W.M. Kürschner, Paleoatmospheric signatures in Neogene fossils leaves, Science 260 (1993) 1788–1790.
[31] W.M. Kürschner, J. Van der Burgh, H. Visscher, D.L. Dilcher, Oak leaves as biosensors of late Neogene and early Pleistocene paleoatmospheric CO_2 concentrations, Mar. Micropaleontol. 27 (1996) 299–312.
[32] A.M. Haywood, Evaluating General Circulation Climate Model Reliability Against the Pliocene Geological Record, PhD Thesis, Reading University, Reading, UK, 2001, 295 pp.
[33] T.F. Stocker, Past and future reorganizations in the climate system, Quat. Sci. Rev. 19 (2000) 301–319.
[34] W.S. Broecker, G.H. Denton, The role of ocean atmosphere reorganizations in glacial cycles, Geochem. Cosmochem. Acta 53 (1989) 2465–2501.
[35] A. Stössel, S.J. Kim, S.S. Drijfhout, The impact of Southern Ocean sea ice in a global ocean model, J. Phys. Oceanogr. 28 (1998) 1999–2018.
[36] C. Gordon, C. Cooper, C.A. Senior, H. Banks, J.M. Gregory, T.C. Johns, J.F.B. Mitchell, R.A. Wood, The simulation of SST, sea ice extents and ocean heat transports in a version of the Hadley Centre coupled model without flux adjustments, Clim. Dyn. 16 (2000) 147–168.
[37] J.M. Gregory, J.F.B. Mitchell, The climate response to CO_2 of the Hadley Centre coupled AOGCM with and without flux adjustment, Geophys. Res. Lett. 24 (1997) 1943–1946.
[38] J.M. Edwards, A. Slingo, Studies with a flexible new radiation code 1: Choosing a configuration for a large-scale model, Q.J.R. Meteorol. Soc. 122 (1996) 689–719.
[39] S. Cusack, J. Slingo, J.M. Edwards, M. Wild, The radiative impact of a simple aerosol climatology on the Hadley Centre GCM, Q.J.R. Meteorol. Soc. 124 (1998) 2517–2526.
[40] D. Gregory, R. Kershaw, P.M. Inness, Parametrisation of momentum transport by convection II: tests in single column and general circulation models, Q.J.R. Meteorol. Soc. 123 (1997) 1153–1183.
[41] P. Cox, P.R. Betts, C. Bunton, R. Essery, P.R. Rowntree, J. Smith, The impact of new land-surface physics on the GCM simulation and climate sensitivity, Clim. Dyn. 15 (1999) 183–203.
[42] P.R. Gent, J.C. McWilliams, Isopycnal mixing in ocean circulation models, J. Phys. Oceanogr. 20 (1990) 150–155.
[43] H. Cattle, J. Crossley, Modelling Arctic climate change, Phil. Trans. R. Soc. Lond. A 352 (1995) 201–213.
[44] W.A. Berggren, D.V. Kent, C.C. Swisher, M.P. Aubry, A revised Cenozoic geochronology and chronostratigraphy, in: W.A. Berggren, D.V. Kent, M.P. Aubry, J. Hardenbol (Eds.), Geochronology, Time Scales and Global Stratigraphic Correlation, Tulsa, Soc. Sediment. Geol. Spec. Publ. 54 (1995) 129–212.
[45] E.M. Brouwers, Late Pliocene paleoecologic reconstructions based on ostracode assemblages from the Sagavanirktok and Gubik Formations, Alaskan North Slope, Arctic 47 (1994) 16–33.
[46] T.M. Cronin, R.C. Whatley, A. Wood, A. Tsukagoshi, N. Ikeya, E.M. Brouwers, W.M. Briggs, Microfaunal evidence for elevated mid-Pliocene temperatures in the Arctic Ocean, Paleoceanography 8 (1993) 161–173.
[47] A.C. Ravelo, D.H. Andreasen, Enhanced circulation during a warm period, Geophys. Res. Lett. 27 (2000) 1001–1004.
[48] D. Rind, M. Chandler, Increased ocean heat transports and warmer climate, J. Geophys. Res. 96 (1991) 7437–7461.
[49] R.W. Reynolds, T.M. Smith, A high resolution global sea surface temperature climatology, J. Climatol. 8 (1995) 1571–1583.